Macromolecules

ARTICLE

pubs.acs.org/Macromolecules

Flow Activation Volume in Composites of Polystyrene and Multiwall Carbon Nanotubes with and without Functionalization

José A. Martins,[†,‡,*] Vera S. Cruz,[†,‡] and M. Conceição Paiva[†,§]

[†]Departamento de Engenharia de Polímeros, Universidade do Minho, Campus de Azurém, 4800-058 Guimarães, Portugal

[‡]CICECO, Universidade de Aveiro, 3810-193 Aveiro, Portugal

[§]Instituto de Polímeros e Compósitos/I3N, Universidade do Minho, Campus de Azurém, 4800-058 Guimarães, Portugal

Supporting Information

ABSTRACT: A new experimental protocol for the evaluation of the flow activation volume is proposed. It is based on step-shear experiments carried out on polymer melts. The flow activation volume evaluated agrees with the volume of a tube confining the chain, and is the same for the polymer melt and its composites with as received and functionalized carbon nanotubes. The functional groups bonded to the carbon nanotubes surface facilitate the polymer melt flow, eliminating the solid-like behavior in the high temperature flow region. A model for the morphology of polymer melts with carbon nanotubes is discussed. Polymer−nanotube interaction energies are discussed and the relaxation time of these interactions is estimated. The link between the solid-like behavior at the flow region and the strong shear thinning observed for the carbon nanotube composites is explained analyzing the different response to shear flow of each of the three networks considered by a model for the morphology of these composites.

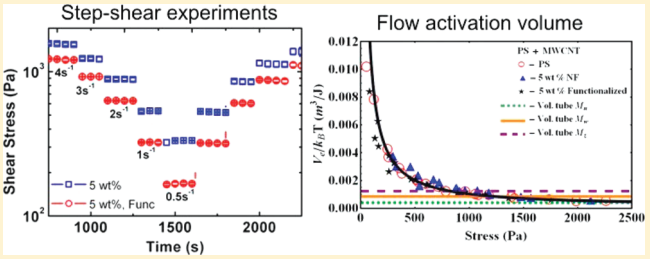

1. INTRODUCTION

Understanding the flow mechanisms in polymer melts and how they are affected by the presence of fillers or nanofillers is crucial for flow modeling. Recent works reported important changes in the polymer melt rheology upon the addition of nanofillers.[1−7] These changes may be affected by the flow field intensity[8,9] and by the dispersion of the nanofillers within the polymer matrix.[4,10] The nanofiller dispersion may be improved by the functionalization of the fillers surface[10,11] and/or by increasing the flow field intensity. Any of these actions affect the rheological behavior of the composite.

Among the changes in the flow behavior reported for composites containing nanofillers and polymer melts is the development of elasticity at the high temperature flow region which is always associated with a strong shear thinning behavior of the composite melt.[1,2,4] The appearance of this solid-like behavior depends on the filler concentration and on its dispersion. Higher melt temperatures and/or good dispersion of the fillers shifts the display of solid-like behavior toward lower filler concentrations.[4,11]

The practical consequence of the appearance of solid-like behavior in nanocomposite melts is the strong increase of their viscosity, which is prominent at low shear rates and at the start-up of flow.[2,4,11] Devising strategies to avoid the emergence of elasticity at the flow region in nanocomposites, while maintaining the properties induced by the nanoparticles at a concentration above the percolation threshold, appears to be a promising route to facilitate both the composite processing and the dispersion of the nanoparticles in the polymer melt.

Another observation reported in the literature is the suppression of the die-swell effect[2] and a drop in the viscosity of nanoparticle filled polymer melts[1,3,6] upon addition of a small concentration of the nanofiller to the polymer melt, affecting the composite processing. Specifically, it was found that the incorporation of ∼0.2 wt % of multiwall carbon nanotubes (CNT) in the polymer melt broadened the temperature interval for extrusion processing and decreased the wall shear stress, which was attributed to "the enlarged effective entanglement distances between adsorbed chains (to the melt-wall interface) and free chains in the melt, because CNT can enhance chain alignment during shear flow".[6]

The changes in rheological behavior and their impact on the processing of nanocomposites may be clarified after understanding how the nanofillers affect the flow of polymer chains at the molecular scale. In this work we evaluate the flow activation volume in a melt of atactic polystyrene (aPS) at the flow region and compare the result with that obtained with composites containing different concentrations of functionalized and as received multiwall CNT. For this evaluation a new experimental protocol was implemented, consisting on imposing small perturbations to a monotonic melt shear test and analyzing the response of the melt to the perturbations. The flow activation volume was evaluated by applying the rate theory of plastic

Received: August 8, 2011
Revised: October 4, 2011
Published: November 23, 2011

deformation which relates the response of the melt to the induced perturbations.[12,13] A brief summary of this theory and of its main assumptions is presented next.

In the rate theory of plastic deformation, the activation volume is related to the distance needed to move the *flow segment* from the reactant to the activated state. If the energy barrier for dislocation of flow segments in the flow direction, in the absence of a stress, is ΔG_o, then the strain rate resulting from a shear stress τ is given by

$$\dot{\gamma}(\tau, T) = \dot{\gamma}_0 \exp[-(\Delta G_o - \tau V^*)/k_B T] \quad (1)$$

where $\dot{\gamma}_0$ is a constant, k_B the Boltzmann constant, V^* is the activation volume, and T the absolute temperature. From this equation the flow activation volume is expressed as

$$V^* = k_B T \frac{d[\ln(\dot{\gamma})]}{d\tau} \quad (2)$$

An experimental, *or apparent*, flow activation volume may thus be evaluated by measuring the material's response to perturbations of a monotonic test, assuming that the deformation mechanism imposed by the monotonic test remains unaltered by the perturbations. A possible monotonic test consists of applying a deformation at constant shear rate, $\dot{\gamma}$. Perturbations are small variations of the shear rate that are maintained during short-time intervals, a couple of seconds. The material's response is the recorded shear stress values (τ) at each strain rate, that of the monotonic test and those of the perturbations. The experimental, or apparent, flow activation volume is then evaluated at constant temperature as

$$V_e = k_B T \left[\frac{d[\ln(\dot{\gamma})]}{d\tau}\right]_{T, DefMech} \quad (3)$$

under the assumption of constant deformation mechanism.

The experimental and true flow activation volumes, V_e and V^*, respectively, are different. A relationship between them is obtained considering both forward and backward transitions over the energy barrier and rewriting eq 2 in a more general form as

$$\dot{\gamma}(\tau, T) = 2A \sinh[\tau V^*/k_B T] \quad (4)$$

where $A = \dot{\gamma}_0 \exp[-\Delta G_o/k_B T]$. Inserting this equation into eq 3, we obtain the relationship between V_e and V^* [12]

$$\frac{V_e}{k_B T} = \frac{V^*}{k_B T} \coth(\tau V^*/k_B T) = \alpha \coth(\tau \alpha) \quad (5)$$

where $\alpha = V^*/k_B T$ is the only fitting parameter to the experimental data. This last equation was derived under the additional assumption that, for very large values of τ, $\partial V^*/\partial \tau = 0$.

The flow activation volume estimates obtained using this theory elucidated the deformation mechanisms in metals and received experimental confirmation by in situ observations of dislocations moving in a sample strained in a transmission electron microscope or in an synchrotron beam.[13] Possible deformation mechanisms considered in the plastic deformation of metals and alloys included the climb mechanism, the Piersl−Nabarro mechanism and the nonconservative motion of jogs.[12] The corresponding values of flow activation volume are $1b^3$, $10b^3$ to 10^2b^3 and 10^2b^3 to 10^4b^3, respectively, where b is the Burgers vector. Since $b \sim$ Å, the above flow activation volumes may vary from $\sim$3 Å^3 up to $\sim 10^4$ Å^3. Flow activation volumes evaluated for deformation processes of solid polymers are around 10^4 Å^3 and involve the movement of $\sim$200 carbon atoms of the main chain.[14]

A similar application of the theory was made in compression studies of polyethylene crystals of different thickness produced by compression molding.[14] In these experiments, positive and negative strain rate jumps, for example from 5.5×10^{-3} s^{-1} to 5.5×10^{-2} s^{-1} and the opposite, were applied to PE samples. A constant flow activation volume of 8.4×10^3 Å^3 was evaluated for crystals thicker than 40 nm, while the yield stress increases with the lamellae thickness. The apparent independence of flow activation volume on crystal thickness for crystals thicker than 40 nm was explained by the prevalence in the thicker crystals of mechanisms such as edge and screw dislocations that start governing the strain rate.

We imported the words "*flow mechanisms*" from these works and its meaning has to be modified to describe the flow of polymer melts. In the viscoelastic linear regime, the following combination of mechanisms were considered to explain the stress relaxation of a tube deformed during an idealized rapid "step" deformation: chain reptation, primitive path (or contour length) fluctuations, Rouse modes inside the tube and (thermal) constraint release (CR). For fast flows, in the viscoelastic nonlinear regime, two additional tube relaxation mechanisms were considered. Under flow, chains stretch, relaxing by retraction, which originates an additional release of constraints, the convective constraint release, a mechanism similar to the thermal constraint release, but in this case originated by flow. Since at steady state chains are no longer stretching, the convective release of constraints imposed by the matrix chains on the test chain should proceed at a rate proportional to the flow rate. At steady-state, it is also considered that, for shear rates higher than τ_R^{-1}, the Rouse relaxation time of the chain, convective constraint release (CCR) dominates over reptation inducing chain reorientation and eventually tube dilation.[15,16]

The flow activation volume in polymer melts may, or may not, be sensitive to these different mechanisms. Hence, the words "flow mechanism" should be replaced by "*volume of the flow unit activated by flow*". It is this volume that is evaluated with eq 5. Since we will limit our experiments to shear rates below the reciprocal of the longest relaxation time, much below τ_R^{-1}, the tube dilation mechanism is excluded and the largest physically meaningful volume to consider is that of a tube confining the chain, and the lowest is that of a Kuhn monomer.

The volume of a tube confining a chain with molecular weight M is

$$V_t = \pi \frac{a^3}{4} Z = \frac{\pi}{4} \frac{M_e^{1/2}}{M_k^{3/2}} l_k^3 M \quad (6)$$

where a is the tube diameter defined as $\langle a^2 \rangle = n_{k,e} l_k^2$ and M the chain's molecular weight; $n_{k,e}$ is the number of statistical chain segments between entanglements, each one having a length equal to one Kuhn monomer (l_k); Z is the number of entanglements in the chain defined by the ratio M/M_e, where M_e is the molecular weight between entanglements; and M_k is the molecular weight of the Kuhn monomer.

The physical volume of the chain inside the tube may be evaluated from the packing length definition,[17] which is

$$p = \frac{V_{chain}}{\langle r^2 \rangle_0} \quad (7)$$

where V_{chain} is the physical volume of the chain and $\langle r^2 \rangle_0$ the average square end-to-end distance of the unperturbed chain.

Table 1. Molecular Characteristics of the Polystyrene Used in This Work: Weight Average Molecular Weight, M_w, z Average Molecular Weight, M_z, Polydispersity Index, M_w/M_n, Molecular Weight between Entanglements, M_e, Molecular Weight of the Kuhn Monomer, M_k, Length of the Kuhn Monomer, l_k, Volume of a Tube Confining a Chain with Molecular Weight of M_n and Physical Volume of a Chain with Molecular Weight M_n, $V_{chain\text{-}M_n}$ [a]

	M_w (kg/mol)	M_z (kg/mol)	M_w/M_n	M_e (g/mol)	M_k (g/mol)	l_k (Å)	$V_{tube\text{-}M_n} \times 10^{-6}$ (Å^3)	$V_{chain\text{-}M_n} \times 10^{-5}$ (Å^3)
aPS	205.0	298.0	2.1	14 800	710	18	2.88	1.75

[a] Data were extracted from refs 17 and 18.

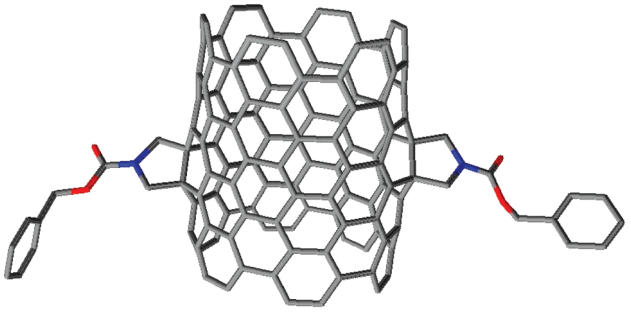

Figure 1. Surface density of functional groups bonded to the CNT.

Using the self-similarity property of Gaussian chains, with $V_{chain} = n_k v_k$, where v_k is the volume of one Kuhn monomer and $\langle r^2 \rangle_0 = n_k l_k^2$, the above equation allows also the volume of one Kuhn monomer to be evaluated as $v_k = p l_k^2$.

2. EXPERIMENT

2.1. Polymer Samples. The properties of the atactic polystyrene used are presented in Table 1. Its T_g evaluated at 10 °C/min, preceded by a cooling at the same rate, was 91 °C. Values of the molecular weight between entanglements, molecular weight of the Kuhn monomer and its length were obtained from references17 and18. Procedures for evaluating the volume of a chain and the volume of one Kuhn monomer were presented above. Samples for the rheological experiments were prepared from pellets melted at 200 °C and injected into a mold using a Thermo Scientific Mini Jet II injector. The mold temperature was set to 100 °C, and the injection conditions were: pressure at 400 bar applied during 13 s, and second pressure at 200 bar applied during 4 s.

2.2. Surface Functionalization of the Nanotubes. The CNT used were NC7000 produced by Nanocyl with average diameter and length of 9.5 nm and 1.5 μm, respectively, containing 90% CNT and 10% of impurities such as metal oxides and catalyst. The CNT were chemically functionalized using the 1,3-dipolar cycloaddition reaction, following the procedure described in a previous study.[19] This functionalizatioin does not involve oxidizing acid treatments. It is a mild chemical procedure that does not induce CNT breakage. The reaction was carried out under solvent free conditions at 180 °C during 1 h. According to previous studies,[19] these conditions lead to a yield of approximately 1.5% of functional groups (measured as the number of functional groups relative to C atoms) formed by a cyclic amine (pyrrolidine) substituted with the benzyloxycarbonyl group. The functionalization degree attained corresponds to approximately one functional group per 60 C atoms at the CNT surface, equivalent to one functional group for the area of a rectangle formed by 7 × 3 C hexagons. The approximate surface density of functional groups on the CNT outer graphene layer is depicted in Figure 1.

2.3. Preparation of the Composites. The preparation of the composites followed a protocol similar to that described in other published works.[20] The above nanotubes, as received and functionalized, were melt mixed with polystyrene in a Brabender mixer (Plastograph EC) at 180 °C during 30 min at 100 rpm. The concentration of nanotubes in the composites were 1.25, 5, and 15 wt %. Collected samples were further heated at 200 °C and injected into a mold following the procedure described above for polystyrene.

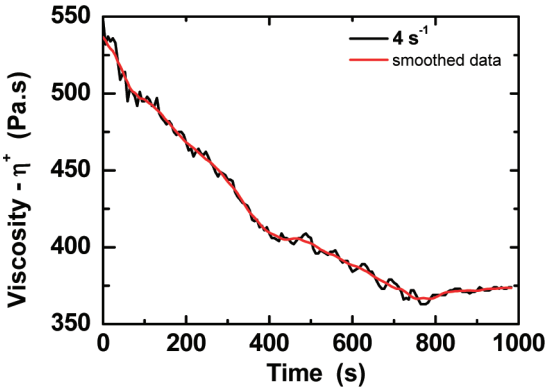

Figure 2. Start-up of shear experiment with aPS sheared with a constant rate of 4 s^{-1} at 220 °C. The melt viscosity, or shear stress, increases initially up to a maximum at low strain values, decreases and stabilizes at a nearly constant value after a shearing time of ≈800 s. Red line shows smoothing of the data using the adjacent averaging of five points.

2.4. Step-Shear Experiments. The shear experiments were performed in a Physica MCR 300 rheometer (Paar Physica) with parallel plate configuration (plate diameter 25 mm and gap size set to 0.7 mm) and cone-and-plate configuration (plate diameter 25 mm and cone angle 2°). They were preceded by all recommended calibrations. A set of reference experiments were performed under nitrogen atmosphere at the flow rate recommended by the manufacturer and compared with experiments performed in air. Experiments with different samples were performed for each condition and exceptionally different results, which could result from slippage or other experimental artifacts, were rejected. The results reported represent the average of a set of five experiments.

The protocol followed in the step-shear experiments was based on results of previous works where the strain needed to establish a melt state with nearly constant viscosity at different melt temperatures was evaluated.[21] For aPS, as shown in Figure 2, the melt at 220 °C, sheared with a constant rate of 4 s^{-1}, attains a state of nearly constant viscosity after ≈800 s of shearing time. This was the first step of the step-shear experiments described in this work, although steps with different shear rates (above or below 4 s^{-1}) could also be considered. However, they should always be limited to shear rates below the reciprocal of the longest relaxation time. This test was perturbed by shear steps of lower shear rates (3 s^{-1}, 2 s^{-1}, 1 s^{-1}, 0.5 s^{-1}, and up, back to 4 s^{-1}), each one with a time duration of 180 s.

In the language of the rate theory of plastic deformation the first step is the monotonic test and the shear steps are perturbations induced to that test. An assumption of this theory is that the flow mechanism of the monotonic test, in other words, the true volume of the flow unit activated by flow was unaffected by the perturbations induced during the shear steps.

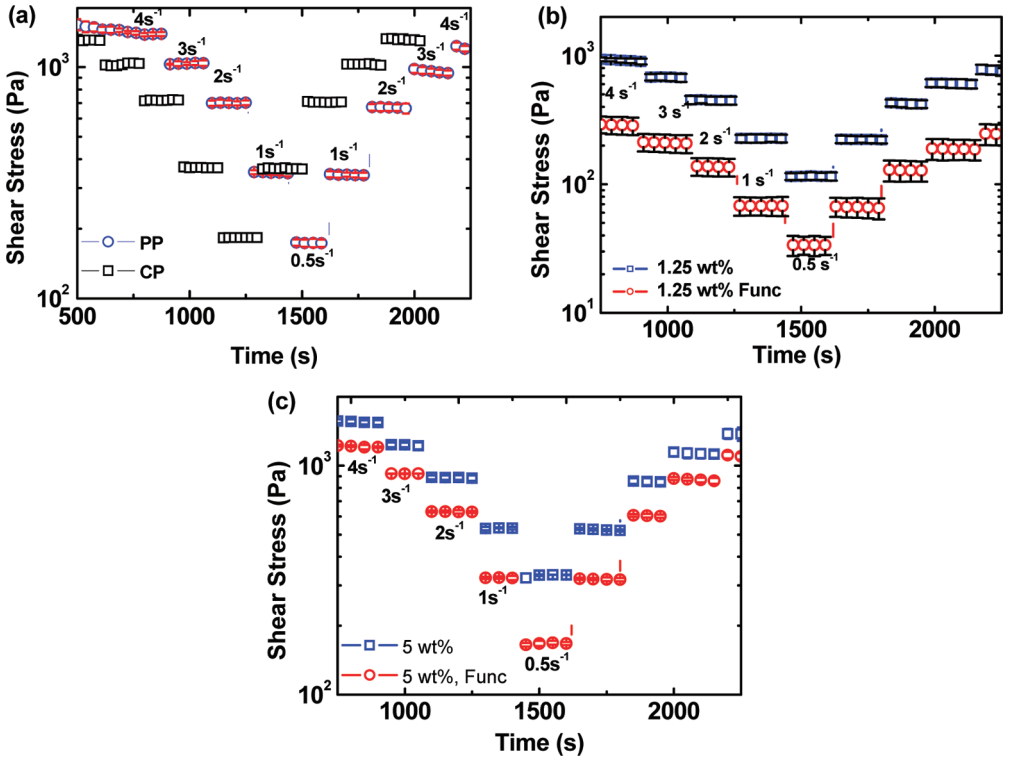

Figure 3. Results of step-shear experiments. (a) Atactic polystyrene at 220 °C with the parallel plate configuration (PP), pate diameter of 25 mm and gap size of 0.7 mm and cone-and-plate configuration (CP), plate diameter of 25 mm and cone angle 2°. For the PP configuration, the shear starts with a constant rate of 4 s^{-1} during 800 s (strain of 3200 s.u.) until the attainment of a well-defined steady-state. The monotonic test was perturbed with the following shear steps: 3 s^{-1}, 2 s^{-1}, 1 s^{-1}, and 0.5 s^{-1} and up again. The time duration of each step was 180 s. The time duration of the initial shearing step for the cone-and-plate configuration was 600 s. (b) Similar protocol as in part a with the PP configuration for the composite with 1.25 wt % of CNT with and without functionalization, circles and squares, respectively. The temperature of the experiment was 220 °C. (c) The same as in part b for the composite with 5 wt % of CNT, functionalized (half-filled circles) and unfunctionalized (half-filled squares). Same temperature as in part b.

For this reason, the first step of step-shear experiments was performed at a low shear rate, within the lower Newtonian plateau region, and perturbations were applied at still lower shear rates during short-time intervals. Because of the shear-thinning behavior of polymer melts, perturbations of an experiment carried out at shear rates higher than the longest relaxation time would imply significant changes of the melt viscosity which does not guarantee that the volume of the flow unit would remain unaffected by the perturbations.

3. RESULTS AND DISCUSSION

We start by presenting and discussing the results obtained on the step-shear experiments. These results are then used to evaluate the flow activation volume of the polymer and composites. A model proposed by Pötschke et al.,[4] describing the interactions in composite melts, is discussed, namely: (i) its ability to explain the observed solid-like behavior at the flow region shown by the composites with higher concentration of CNT, (ii) the coupling of this behavior to the strong shear thinning, and (iii) the adequacy of this model to the similar flow activation volumes evaluated for the polymer melt and the composites. Values for the relative strength of the interactions involved and their relaxation time are also provided in the final section.

3.1. Step-Shear Experiments. Figure 3 shows the results of step-shear experiments following the protocol described above. For aPS, Figure 3a shows similar results for the parallel plate and cone-and-plate configurations. Regardless the configuration used, the same value of shear stress was measured for shear steps at the same rate. The first step consisted of a shearing at 4 s^{-1} that was applied during a length of time to ensure the establishment of melt state with nearly constant viscosity. Results in Figure 2 indicated that, at 220 °C, a melt state with nearly constant viscosity was achieved after a shearing time of ~800 s. Similar experiments, performed at different melt temperatures, were used to establish the time duration of the first step at those temperatures.[21]

Differences in the time duration of the first step for experiments performed with the parallel plate and cone-and-plate configurations are explained by the differences between the nominal shear rate and its average value in these two configurations. Because in the cone-and-plate configuration the shear rate is constant along the plate radius and in the plate−plate configuration its average value is 2/3 the shear rate value at the edge of the plate, the shearing time required to establish a melt state with nearly constant viscosity in the cone-and-plate configuration is ~2/3 that used for the parallel-plate configuration.

Regardless the configuration used, once the viscosity of the monotonic test stabilized at a constant value, small perturbations to this test were applied in steps with time duration of 180 s at lower shear rates. Results of these perturbations are presented in Figure 3a for aPS and in Figures 3b and 3c for the composites with 1.25 and 5 wt % of CNTs, respectively. The similar shear stress values obtained for the same shear rates when the

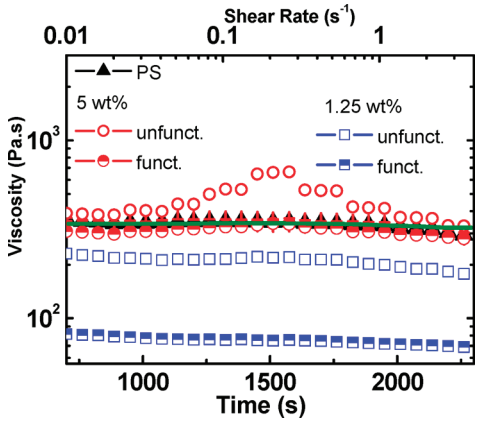

Figure 4. Variation of melt viscosity with time during the perturbation of the monotonic test at 220 °C with the shear steps of Figure 3. Filled triangles are the results obtained for polystyrene. Squares indicate the results obtained for the composites with 1.25 wt % of nanotubes: functionalized nanotubes (half-filled squares); unfunctionalized nanotubes (unfilled squares). Circles are the results obtained for the composites with 5 wt % of nanotubes. Solid line shows the viscosity variation with shear rate. The melt was initially sheared with constant rate of 4 s^{-1} during 800 s with the same strain as in Figure 3. After this shearing, a controlled shear rate was performed from 4 to 0.01 s^{-1}.

experiment was carried out at decreasing or increasing strain rate steps confirmed that the flow mechanism was unperturbed by the applied shear steps. In other words, it remains within the viscoelastic linear domain. Greater differences in the stress values were measured for the initial and final steps, but they are within the experimental error.

3.1.1. The decrease in the viscosity of the composites with low concentration of CNT. Results of step-shear experiments obtained for the composites with a 1.25 wt % of CNT shown in Figure 3b indicate a decrease in the melt viscosity relative to the polymer (open and half-filled squares). This decrease is more significant for the composite with functionalized CNT, and is confirmed by the results of Figure 4 (half-filled squares). As reported in other works,[1,3,6] this behavior contradicts the classical Einstein equation for the viscosity of a liquid in which a large number of spheres are suspended in irregular distribution.[22] This viscosity decrease was reported by Mackay et al. for composites of cross-linked PS nanoparticles and atactic polystyrene.[1] Jain et al. reported a similar effect in composites of silica nanoparticles and isotactic polypropylene.[3] The same effect was also reported by Xu, Lele, and Rastogi for composites of carbon black, or MWCNT, and linear polyethylene.[6]

At least two interpretations for this behavior were presented, one assigning it to an increase in free volume and configurational changes[1] and the other to the selective adsorption of high molecular weight polymer chains on the nanofillers surface.[3] From our point of view, these two interpretations are not necessarily exclusive. Fluctuations of chain ends on the adsorbed chains may induce an excluded free volume around the nanoparticles. This assumption is justified below.

Mackay et al. explained initially the viscosity decrease by a free volume increase, although other possible effects were not excluded.[1,23] They considered that because in their study the nanoparticles and polymer melt were chemically the same, with similar refractive indexes, dispersion forces were minimized.[1,24] In latter works two design parameters were enunciated that could cause a viscosity reduction in the composites: (i) the polymer molecular weight should be above the critical molecular weight, and (ii) the interparticle half-gap should be less than the polymer coil size (R_g).[25]

Because a significant reduction in the viscosity was observed without noticeable changes in the plateau modulus, the authors concluded that the average number of entanglements in the melt was preserved. Accordingly, the mechanism responsible for the viscosity decrease could not be associated with changes in the plateau modulus.[23] Besides the free volume increase, constraint release caused by the addition of the nanoparticles was then proposed as an additional mechanism responsible for that effect.

At this point it is worth to mention the work of Jain et al.[3] where an acceleration of the crystallization kinetics in composites of iPP and silica nanoparticles was reported, together with a decrease in the viscosity of the melts. Since this acceleration can only be understood if silica nanoparticles act as nucleating agents, implying interactions between iPP and the nanoparticles, the increase in the free volume was excluded for explaining the observed viscosity decrease. Instead, it was assigned to the selective adsorption of high molecular weight polymer chains on the surface of the fillers. The mechanism by which this selective adsorption contributed to the viscosity decrease was not explained, but a reasoning involving the interparticle distance and the coil size, similar to the design parameter mentioned above,[25] was presented.

It is a fact that most published research work on the solidification of composites of inorganic nanoparticles, including CNT, and isotactic or syndiotactic polymer melts, report the acceleration of crystallization kinetics upon the inclusion of the nanoparticles. Thus, considering that chain segments of polymer melts interact with the nanoparticles is an intuitive assumption, even when the composites involve atactic polymer melts. In this case, studies with aPS reported that syndiotactic conformational sequences of chain segments were present in the predominantly atactic polymer.[26]

Since a viscosity decrease may be interpreted through a free volume increase, one has to search for physically realistic mechanisms, consistent with available experimental results, which could explain that increase. Following Mackay et al.,[23,25] only chains with molecular weight above M_c may interact with the nanoparticles, and the probability of interaction increases with the chain molecular weight.[3] Thus, for the composites with low concentration of nanoparticles, where the viscosity decrease is observed, we consider that only the longest chains in the melt interact with the nanoparticles.[3]

The longest relaxation time of the chain is affected, besides reptation of the primitive chain inside the tube, by contour length fluctuations. The results presented in the Supporting Information, Figure SI.1, indicate that the longest relaxation time of the composite with 1.25 wt % of CNT is much shorter than the chain's longest relaxation time of ≈0.01 s. These results suggest an increase of the number of chain segments between entanglements, or M_e, and thus the decrease of chain entanglements.

We may also consider, based on our results and on ref 3, that the longest chains interacting with the nanoparticles (or adsorbed on their surfaces) are less entangled than the chains of similar molecular weight in the bulk melt. The relative contour length fluctuation amplitude may be estimated as $\delta\bar{L}/\bar{L} \cong 1/\sqrt{Z}$,[27,28] where $\delta\bar{L}$, $\bar{L}$, and Z are, respectively, the average of the fluctuation, the average contour length of the primitive chain, and the number of entanglements in the chain. .Thus, the chains

interacting with the nanoparticles present larger relative contour length fluctuation amplitudes. They may explain the increase of free volume, hence the lower viscosity of the melts, explaining also the decrease of the longest relaxation time for the composites with low concentration of nanoparticles. The effect of melt viscosity increase observed for the composites with higher CNT concentration, and the low-frequency "solid-like" elasticity is discussed in section 3.3.2.

As for the viscosity decrease observed in composites with low concentration of functionalized nanotubes, we consider that the free volume increases as a result of two contributions: one is promoted by the functional groups attached to the polymer chains and it is observed only in composites with functionalized CNT having a functionalization type similar to that used in the present work; the other results from fluctuations of chains ends in the adsorbed chains. This may be the only contribution for the free volume increase in nonfunctionalized CNT, although it may contribute also to the free volume increase in functionalized CNT. In this case, the extend of chain adsorption must be lower than that occurring in CNT with nonfunctionalized surfaces.

3.1.2. Effect of Perturbations on the Volume of the Flow Unit. The step-shear experiments on composites with 5 wt % CNT shown in Figure 3c yielded similar results to those obtained for the pure polymer. Differences in the polymer and composite melts' flow behavior are better illustrated in Figure 4. It shows the viscosity variation during the shear steps for aPS and its composites. The viscosity of aPS is almost constant during the whole perturbation (triangles). It is in agreement with the viscosity measured on a controlled shear rate experiment carried out from 4 to 0.01 s^{-1} after preshearing the melt at 220 °C with the rate of 4 s^{-1} during 800 s (solid line in Figure 4).

The conclusion expressed by these results is that the perturbations (shear steps) induced to the monotonic test did not influence the melt viscosity. This result may tempt us to conclude that also the flow mechanism (true volume of the flow unit activated by flow) was unaffected by the perturbations. However, this last conclusion has implicit an unproved association, which is that a specific viscosity value is solely determined by a unique flow mechanism and, consequently, that differences in viscosity result from the action of different flow mechanisms. This is an important discussion that we will continue below.

As discussed above, the viscosity values obtained for the composites with 1.25 wt % CNT, either functionalized or nonfunctionalized, is lower than that of aPS while that of the composites with 5 wt % of functionalized CNT is also constant and similar to that of aPS. There is a clear indication however that the shear steps affected the melt viscosity of the composite with 5 wt % of nonfunctionalized CNT. It remains to be clarified if this variation affected, or not, the volume of the flow unit. A discussion made in the last section based on a model proposed by Pötschke et al.[4] and the quantitative evaluation of the flow activation volume made in the next section, suggest, also in this case, that the volume of the flow unit was not affected by the perturbations.

It is widely known from experimental results obtained for composites with high concentration of CNT that, besides the "solid-like" elasticity at the flow region, they also show a strong shear thinning behavior. Changes of viscosity observed during the perturbations result from the strong shear thinning. Therefore, we may anticipate that similar variations in the viscosity during the perturbations would be obtained for the aPS melt, or

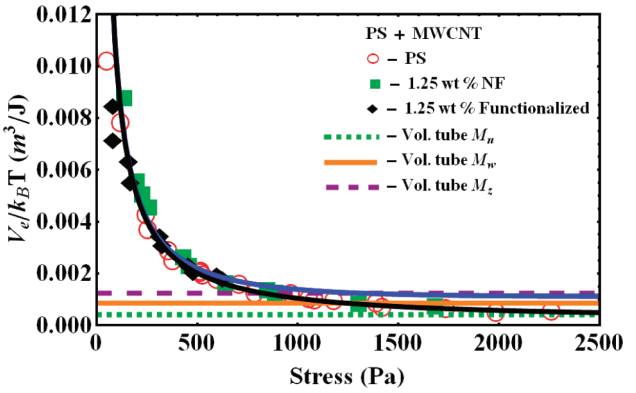

Figure 5. Variation of the flow activation volume with the shear stress for polystyrene and the composites with 1.25 wt % of CNT nonfunctionalized (NF) and functionalized. Black line is the fit of polystyrene experimental data obtained with the equation derived from the rate theory of plastic deformation, eq 5. The blue line represents a similar fit to the results of the composite with 1.25 wt % of functionalized nanotubes. As shown in the plot, horizontal lines represent the volume of a tube confining the chains with M_z, M_w, and M_n.

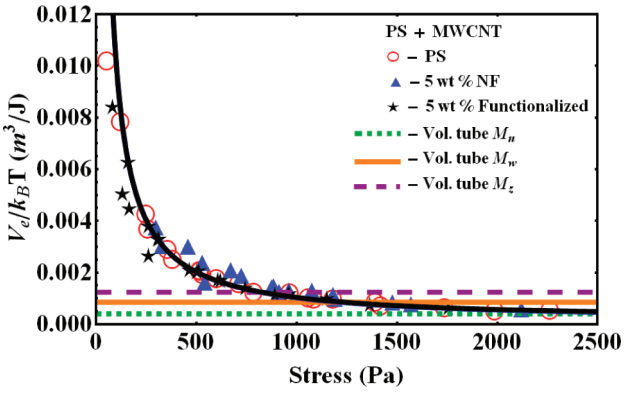

Figure 6. Variation of the flow activation volume with the shear stress for polystyrene and the composites with 5 wt % of nanotubes. Black line is the fit of polystyrene experimental data obtained with the equation derived from the rate theory of plastic deformation, eq 5.

any other polymer melt, if the first shearing step was performed at a higher shear rate. However, experiments at high shear rates are also prone to experimental errors resulting from flow instability which may result in mass loss, slippage and other effects. For this reason also, we limited the first step in the step-shear experiments to a low shear rate value.

3.2. Flow Activation Volume. From eq 3, it is observed that the experimental flow activation volume is simply the slope in curves of $\ln(\dot{\gamma})$ versus the shear stress, obtained from the data in Figure 3. Plots of these curves are provided as Supporting Information in Figure SI.2. The derivatives are presented in Figures 5 and 6 for the composites with 1.25 and 5 wt % of nanotubes, respectively, additionally with results obtained for polystyrene in a broader temperature range. The flow activation volume, obtained from the parameter α in eq 5, was evaluated at 240 °C, the highest temperature at which step-shear experiments were performed. Although step-shear experiments were also performed for composite samples with 15 wt % of nanotubes, their flow activation volume was not evaluated due to the low reproducibility of the experimental results. Probably this is the result of the strong

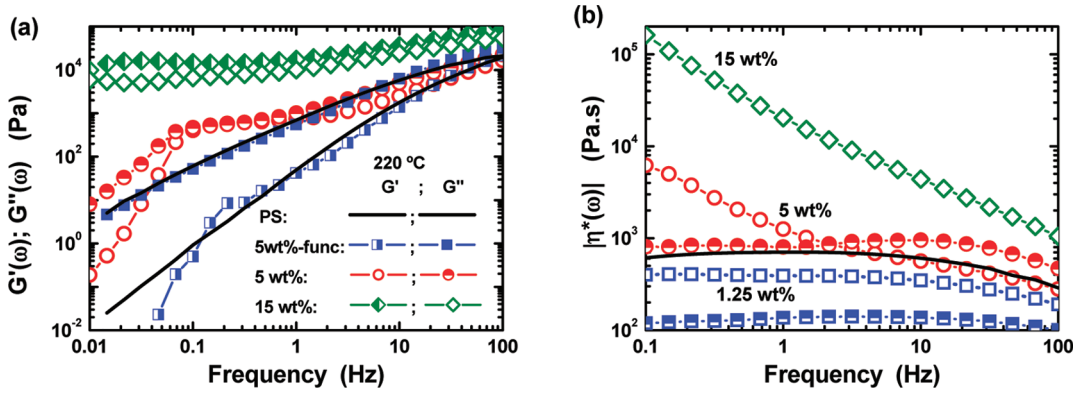

Figure 7. Small amplitude oscillatory shear results for polystyrene and the composites with CNT performed with a constant stress of 600 Pa at 220 °C. All results were obtained within the high temperature flow region. (a) Variation of the elastic and dissipative components of the complex modulus with the oscillation frequency. Note the different behavior for the composites with functionalized and nonfunctionalized nanotubes and the breakup of the solid-like plateau for the composite with 5 wt % of functionalized nanotubes at a frequency of 0.1 Hz (relaxation time 10 s). The polymer longest relaxation time at the same temperature is $\sim 10^{-2}$ s. (b) Complex viscosity variation with the oscillation frequency. Open symbols: composites without functionalization of the nanotubes. Half-filled symbols: composites with functionalization of the nanotubes. The viscosity of the pure polymer is indicated by the solid black line. That of the composites with 1.25 wt % of nanotubes with and without functionalization is indicated by squares, half-filled and open, respectively. Note the increased shear thinning behavior at higher concentrations of nanotubes.

shear thinning behavior of this composite melt. These results are also included in Figure SI.3 as Supporting Information.

It was observed that regardless the composite concentration, the experimental flow activation volumes of both functionalized and nonfunctionalized nanotubes superimposed with those evaluated for polystyrene. Fitting of these results with eq 5 yielded the true flow activation volume. The fit of polystyrene data is indicated in Figures 5 and 6 with a black line. The value obtained for the α parameter was 3.357×10^{-4} m^3/J, corresponding to a flow activation volume of 2.378×10^6 Å^3 at $T = 240$ °C. This value is much larger than the physical volume of the chain that is 1 order of magnitude below (see Table 1). Volumes larger than the physical volume of the chain have to be considered to explain this value. The limiting value of 2.378×10^6 Å^3 is in agreement with the volume of a tube confining a chain with molecular weight M_n, which is indicated by the dotted green line in the Figures 3 and 4. Volumes of a tube confining chains with M_w and M_z are indicated by the horizontal solid and dashed lines, respectively. We note again that results similar to those of Figures 5 and 6 are described in the literature for the plastic deformation of metals.[12,13] However, in this last case, much lower values for the flow activation volume were obtained.

These results suggest that the true flow activation volume in polymer melts and in composites with nanotubes, functionalized or nonfunctionalized, is the volume of a tube confining the chain. An assignment of a specific molecular weight of the chain to the true flow activation volume is impossible to be made with these results. An accurate evaluation requires model polymer samples with narrow molecular weight distribution, and that will be studied in future work.

An example of the difficulty in this assignment is illustrated by the experimental data of the flow activation volume for the composite with 1.25 wt % of functionalized CNT shown in Figure 5 with the blue line. The value estimated from these data for the true flow activation volume is closer to the volume of a tube confining the chains with M_z molecular weight. However, the experimental data superimpose with that of the polymer, and differences in the fitting of aPS and the composite data result from the lack of experimental results for the composite at lower melt temperatures and/or higher stress values. This condition should be fulfilled for physically meaningful true flow activation volumes to be evaluated.[12]

Regardless these difficulties, we may safely conclude that flow activation volume is that of a tube confining the chain whose dimensions are estimated from the theory of Gaussian chains, and that interaction of polymer chains with nanoparticles do not affect the flow activation volume in melts. This is a surprising result since in the composite with 5 wt % CNT these interactions are responsible for a solid-like behavior at the flow region. Furthermore, this solid-like behavior is linked to a strong shear thinning. A model describing the morphology of composites of polymer melts and CNT must consider all these features. A possible model is discussed in the next section.

Though these results point to the validity of the tube model for the composites of polymer melts and CNT, it is clear that additional mechanisms, different from those accepted for polymer melts, have to be considered to explain the rheological behavior of these composites. A similar flow activation volume was evaluated for the composites in the presence and absence of low-frequency "solid-like" elasticity, as well as for the pristine polymer. This elasticity may be explained by a "delayed constraint release mechanism" for the interactions between the polymer melt and the nanotubes. The physical reason for such an assumption is justified below in section 3.3.1.

3.3. The "Solid-Like" Behavior and the Strong Shear Thinning. Polymer/CNT composites typically present a strong shear thinning behavior, especially for composites with high CNT concentration, as depicted in Figure 7. Figure 7a presents results of small amplitude oscillatory shear experiments at the viscoelastic linear regime for the polymer and the composites with 5 wt % of CNT, functionalized and nonfunctionalized. The experiments were performed at 220 °C with a constant stress of 600 Pa, below the viscoelastic linear limit of 1000 Pa. Under these conditions it may be considered at a reasonable approximation that $G'(\omega)$ and $G''(\omega)$ cross at $\approx$100 Hz, indicating that the polymer longest relaxation time is $\sim 10^{-2}$ s.

The behavior of the composite with 5 wt % of functionalized nanotubes is similar to that of the polymer, the only difference

being an incipient elastic plateau for $G'(\omega)$ between 0.2 and 0.5 Hz. The composite with 5 wt % of nonfunctionalized CNT presents the usual elastic plateau at the flow region. Extension of the $G'(\omega)$ and $G''(\omega)$ variation to the lowest accessible experimental frequency range indicates that they cross again at very low frequencies. We consider that this frequency (≈0.08 Hz) marks the end of the solid-like behavior at the flow region. The relaxation time of polymer-nanotube interactions may be estimated from this frequency. Thus, at 220 °C that relaxation time is approximately 12.5 s, 3 orders of magnitude above the longest relaxation time of polymer chains ($\sim 10^{-2}$ s).

Comparison of the results presented in Figure 7a with the complex viscosity variation of Figure 7b allows us to conclude that *the strong shear thinning behavior is linked to the solid-like elasticity at the flow region*. Increasing the oscillation frequency, a viscosity decrease is observed in the frequency window corresponding to the composite solid-like elastic behavior. The results described in parts a and b of Figure 7 have been observed for several polymer systems[1−4] and also for PS-CNT composites.[29] Although the Cox−Merz rule fail for polymer/nanotube composites, steady-state shear measurements in these composites show also a strong shear thinning.[30]

A final note is imposed concerning the differences of viscosity values shown in Figure 7b and Figure 4. The results of Figure 7b were obtained without preshearing of the melt while in Figure 4 the melt was presheared during 800 at 4 s^{-1}. Besides this difference, the failure of Cox−Merz rule explains also the different results obtained for the composites.

3.3.1. A Possible Model for the Melt Morphology of a Carbon Nanotube/Polymer Composite. In order to build a model that explains the results presented in this work it is necessary to know the order of magnitude of the interactions between the nanotubes in the agglomerates, between polymer chains and nanotubes, and the strength of the interactions involving only polymer chain segments. A model considering these interactions was proposed by Pötschke et al.[4] This model considers that blending of polymers with nanotubes results in the formation of three networks: (1) a temporary polymer network formed by entanglements, (2) the carbon nanotube network, and (3) a combined carbon nanotube-polymer network.

According to Girifalco et al.,[31] the cohesive energy of nanotubes with a diameter similar to those used in the present work is approximately 47 kJ/mol for each Å of length overlap between adjacent nanotubes. Considering that the length of a C−C bond in graphene is 1.42 Å, this value is probably an overestimation.

Liao and Li estimated the strength of the interactions between polymer chains and nanotubes using molecular dynamics simulations of polystyrene molecules with different length interacting with graphene.[32] They found an increase of the adhesion energy with the chain length and its stabilization at 21.22 kJ/mol for a chain with 80 repeated units, nearly half the molecular weight between entanglements. This adhesion energy results from van der Waals and electrostatic interactions.

For a carbon nanotube-polystyrene system with no chemical bonding two additional sources of interaction were considered, resulting from the mismatch in the coefficient of thermal expansion of the nanotubes and PS, and the radial deformation of nanotubes induced by atomic interactions. Liao and Li considered also that these last two factors "may be more important in governing the interfacial characteristics in CNT/PS systems". The precise value of the interaction energy between polymer chains and nanotubes was not estimated in this work, but it is probably greater than 21.22 kJ/mol.

The interaction energy involving a loop and chain of polystyrene is ≈1.8 kJ/mol at 200 °C,[24,33] the energy barrier for local and correlated conformational transitions involving one Kuhn monomer is around 75 kJ/mol[34] and the flow activation energy of this aPS is around 92 kJ/mol. The flow activation energy of the composites was not estimated due to the failure of time−temperature superposition.

These estimations and the above evaluations for the relaxation time of polymer−nanotube and polymer−polymer interactions may be applied in the model proposed by Pötschke et al.[4] to explain qualitatively the results of Figure 7 and to interpret the values obtained in this work for the flow activation volume. We start by analyzing the separate response of each of the three types of network to an instantaneous shear step.

3.3.2. The Response of the Networks to an Instantaneous Shear Step. The carbon nanotube network has a pure elastic response with zero phase shift between the shear step and the response to the deformation. If a preferential flow direction is imposed, the network of carbon nanotubes will align instantaneously in the flow direction.[6] It was described in the literature that mild shear flows promote the dispersion of CNT in polymer melts.[9] In this case, the rotational component of the flow may induce the fragmentation of the nanotube aggregates into smaller size aggregates. For low shear rates such as those used in this work, improvement in the dispersion of nanotubes by shear is not expected. Since the melt viscosity is constant at steady state, the average dimension of the aggregates is expected to be constant in that melt state.

The interactions at the polymer/nanotube interface are responsible for the "solid-like" behavior at the flow region and their number is expected to increase with the concentration of nanoparticles. The interactions established between CNT and the polymer chains should "compensate" the decrease in polymer−polymer interactions. Thus, the role of contour length fluctuations in composites exhibiting solid-like elasticity at the flow region should be minimal.

According to molecular dynamics simulations results, chain segments contacting the nanoparticles are preferentially oriented parallel to their surface, retaining a high degree of orientation and conformational order.[35] This network should therefore be responsible for the viscoelastic solid behavior shown by the composite at the flow region.

A possible explanation for the strong shear thinning in these composites is the increase in the free volume due to the detachment of chain segments from the nanotubes as a result of the instantaneous orientation of nanotubes in the flow direction. Stronger deformation rates should be associated with the detachment of chain segments with longer length, generating larger free volume and originating the lower viscosity of the composite.

Polymer−polymer interactions have small magnitude, imparting to the composite the behavior of a viscoelastic fluid.

3.3.3. Additional Discussion on the Model Proposed by Pötschke et al.[4] The similar values obtained for the flow activation volume evaluated for the polymer and composites may be interpreted as follows. As explained above, we may consider that when the composite viscosity is constant in time, the number of chain segments detaching and attaching to the nanotubes is equal. This average number of chain segments must depend on the nanotube concentration and on their dispersion within the matrix. Hence, higher concentration of nanotubes implies more frequent interactions with chain segments, explaining therefore the higher values obtained for the elastic plateau. We may

consider that, similarly to the interactions between polymer chains responsible for the entanglement effects and the elastic plateau, the interactions between polymer chains and CNT are dynamic, being created and destroyed within a time comparable to the relaxation time of polymer−CNT interactions, which is nearly 3 orders of magnitude greater than the longest relaxation time of the polymer chains.

An alternative interpretation of the flow behavior in composites with nanofillers, based on coarse grained computer simulations, considered the particle jamming effects as the source of elasticity at the flow region, inducing slow relaxation of the melt.[36] The large relaxation time for polymer−nanotube interactions estimated in our work, the strength of these interactions, and the atomistic molecular dynamics simulations indicating preferential orientation of the polymer chains parallel to the nanoparticle surface are not consistent with a particle jamming effect. Furthermore, if this effect was significant, the experimental flow activation volume of the composites would not superimpose with the values obtained for the polymer, as shown in Figures 5 and 6.

3.3.4. Role of Surface Functionalization of the Nanotubes. We finally focus our attention on the results obtained for the composites with functionalized CNT. We note specifically the lower melt viscosity observed for the composites with functionalized CNT, and the prolonged lower Newtonian plateau for the composite with 5 wt % functionalized CNT, which is linked to the absence of a strong shear thinning. As depicted in Figure 1, the functional groups on the CNT have a phenyl moiety bonded to a flexible $-CH_2-$ unit, similar to the phenyl groups along the polymer chain. From the chemical point of view, part of the polymer/functionalized CNT interactions have a similarity with the polymer/polymer interactions. Specifically, the phenyl on the functional groups may induce strong $\pi-\pi$ interactions with the polystyrene phenyl groups, and their specific role will be studied in a future work. This type of interaction is not favored for the nonfunctionalized CNT/aPS system, due to the helical distribution of the phenyl groups perpendicularly to the aPS backbone. From the physical point of view, the functional groups anchored to the CNT surface act as spacers between the CNT and the polymer chains, increasing the distance between the polymer chains and the CNT surface, imposing an increase in the free-volume. This helps explaining the decrease in the viscosity of the composite melt. However, the fraction of CNT surface area free from functional groups still interact with the polymer chains in the same way as described above for the nonfunctionalized CNT. We thus expect that this type of surface functionalization helps promoting the flow of composites while preserving the interactions between nanotubes and polymer chains that are essential for the improvement of the physical properties of the composite at room temperature.

4. CONCLUSIONS

A new method to evaluate the flow activation volume in polymer melts was presented and its application to composites with CNTs was illustrated. The method is based on step-shear experiments performed over polymer melts at a melt state with nearly constant viscosity. The perturbations induced to a monotonic test allowed a flow activation volume to be evaluated. The variation of the experimental flow activation volume with the shear stress obeys an equation derived from the rate theory of plastic deformation. The true flow activation volume agrees with the volume of a tube confining the chain. This volume is the same for the polymer and composites, regardless the concentration of nanotubes and the state of their surface, nonfuncionalized or functionalized.

The elasticity at the high temperature flow region is related to the strong shear thinning observed in composites with high CNT concentration. The relaxation time of polymer−nanotube interactions was estimated to be around 3 orders of magnitude greater than the relaxation time of polymer−polymer interactions. On the basis of the model proposed by Pötschke et al.,[4] the above elasticity and the flow activation volume estimated in this work could be interpreted. Future work will include a mathematical formulation for this model and additional experimental routes for the quantification of the strength of the interactions involved.

Although the functionalization procedure of the nanotubes[14] used in this work was initially devised to optimize the interactions with the polymer and improve the nanotube dispersion, it was also found that the solid-like behavior at the flow region was absent even at a CNT concentration above the percolation threshold. The potential of this functionalization procedure to simultaneously decrease the viscosity of the composite, maintaining the interactions with polymer chains, will be explored in future works.

■ ASSOCIATED CONTENT

Supporting Information. Small amplitude oscillatory shear behavior of the composites with low concentration of nanotubes, the representation of step-shear experimental results according to the rate theory of plastic deformation, and step-shear experiments for the composite with 15 wt % of CNT. This material is available free of charge via the Internet at http://pubs.acs.org.

■ AUTHOR INFORMATION

Corresponding Author
*E-mail: jamartins@dep.uminho.pt.

■ ACKNOWLEDGMENT

We acknowledge the Portuguese Foundation for the Science and Technology for funding the project FCOMP-01-0124-FEDER-007151 (PTDC/CTM/68614/2006). Work was supported by the European Community fund FEDER and Project 3599/PPCDT.

■ REFERENCES

(1) Mackay, M. E.; et al. *Nat. Mater.* **2003**, *2*, 762.
(2) Kharchenko, S. B. *Nat. Mater.* **2004**, *3*, 564.
(3) Jain, S.; Goossens, J. G. P.; Peters, G. W. M.; van Duin, M.; Lemstra, P. J. *Soft Matter* **2008**, *4*, 1848.
(4) Pötschke, P.; Abdel-Goada, M.; Aligb, I.; Dudkinb, S.; Lellingerb, D. *Polymer* **2004**, *45*, 8863.
(5) Seira, M.; Masaru, K.; Takashi, N.; Kimiya, G.; Katsuhiko, H. *Macromolecules* **2011**, *44*, 4415.
(6) Xu, H.; Lele, A.; Rastogi, S. *Polymer* **2011**, *52*, 3163.
(7) Abbasi, S.; Carreau, P. J.; Derdouri, A. *Polymer* **2010**, *51*, 922.
(8) Camponeschi, E.; et al. *Langmuir* **2006**, *22*, 1858.
(9) McClory, C.; Pötschke, P.; McNally, T. *Macromol. Mater. Eng.* **2011**, *296*, 59.
(10) Moniruzzaman, M.; Winey, K. I. *Macromolecules* **2006**, *39*, 5194.
(11) Mitchell, C. A.; Bahr, J. L.; Arepalli, B.; Tour, J. M.; Krishnamoorti, R. *Macromolecules* **2002**, *35*, 8825.

(12) Krausz, A. S.; Eyring, H. *Deformation kinetics*: J. Willey & Sons, Inc.: New York, 1975.
(13) Caillard, D.; Martin, J. L. *Thermally activated mechanisms in crystal plasticity*; Pergamon Materials Series 8; Elsevier: Amsterdam, 2003.
(14) Kazmierczak, T.; Galeski, A.; Argon, A. S. *Polymer* **2005**, *46*, 8926.
(15) Dealy, J. M.; Larson, R. G. *Structure and rheology of molten polymers: from structure to flow behavior and back again*: Carl Hanser Verlag: Munich, Germany, 2006.
(16) Watanabe, H. *Prog. Polym. Sci.* **1999**, *24*, 1253.
(17) Fetters, L. J.; Lohse, D. J.; Graessley, W. *J. Polym. Sci., Part B: Polym. Phys.* **1999**, *37*, 1023.
(18) Rubinstein, M.; Colby, R. H. *Polymer Physics*; Oxford Univ. Press: Oxford, U.K., 2003.
(19) Paiva, M. C.; et al. *ACS Nano* **2010**, *4*, 7379.
(20) Pötschke, P.; Bhattacharyya, A. R.; Jamke, A. *Eur. Polym. J.* **2004**, *40*, 137.
(21) Martins, J. A.; Zhang, W.; Brito, A. M. *Macromolecules* **2006**, *39*, 7626.
(22) Einstein, A. *Investigations on the theory of the Brownian movement*; Dover Publications, Inc.: New York, 1956; pp 49−54.
(23) Tuteja, A.; Mackay, M. E.; Hawker, C. J.; Van Horn, B. *Macromolecules* **2005**, *38*, 8000. The relaxation modulus is proportional to $\exp(-t/\tau_d)$, with the longest relaxation time τ_d proportional to $n_k^3/n_{k,e}$. The plateau modulus is proportional to $1/n_{k,e}M_k$. Therefore, to conclude for a possible variation in the number of entanglements, a more sensible choice would have been the evaluation of the relaxation time, and not the plateau modulus. In the works of Mackay, the experimental rheological data allowing to analyse to eventual role of the relaxation time was not presented, as far as we know, and the results published do not allow to extract conclusions on that aspect.
(24) Martins, J. A. *Macromol. Theory Simul.* **2010**, *19*, 360. It can be shown that the van der Waals interaction energy between only two PS Kuhn monomers and a PS nanoparticle, with an average radius similar to that used in the Mackay's works is around 2 kJ/mol higher than the melt thermal energy at 200 °C (3.9 kJ/mol).
(25) Tuteja, A.; Duxbury, P. M.; Mackay, M. E. *Macromolecules* **2007**, *40*, 9427.
(26) Johnson, L. F.; Heatley, F.; Bovey, F. A. *Macromolecules* **1970**, *2*, 175.
(27) Doi, M.; Edwards, S. F. *The theory of polymer dynamics*; Oxford University Press: New York, 1995; p 210.
(28) Lin., Y.-W. *Polymer viscoelasticity: basis, molecular theories and experiments*; World Scientific Publishing Co. Pte. Ltd.: Singapore, 2003; Chapter 9, section 9.2, p 154.
(29) Zhang, Q.; et al. *J. Phys. Chem. B* **2008**, *112*, 12606.
(30) Dijkstra, D. J.; Cirstea, M.; Nakamura, N. *Rheol. Acta* **2010**, *49*, 769.
(31) Girifalco, L. A.; Hodak, M.; Lee, R. S. *Phys. Rev. B* **2000**, *62*, 13104.
(32) Liao, K.; Li, S. *Appl. Phys. Lett.* **2001**, *79*, 4225.
(33) Martins, J. A. *J. Macromol. Sci., Part B* **2011**, *50*, 769.
(34) Khare, R.; Paulaitis, M. E. *Macromolecules* **1995**, *28*, 4495.
(35) Allegra, G.; Raos, G.; Vacatello, M. *Prog. Polym. Sci.* **2008**, *33*, 683. See section 3.4—Structure of the polymer/nanoparticle interface.
(36) Pryamitsyn, V.; Ganesan, V. *Macromolecules* **2006**, *39*, 844.